RESEARCH ARTICLE SUMMARY

MOLECULAR BIOLOGY

E. coli transcription factors regulate promoter activity by a universal, homeostatic mechanism

Vinuselvi Parisutham, Sunil Guharajan, Melina Lian, Md Zulfikar Ali, Hannah Rogers, Shannon Joyce, Mariana Noto Guillen, Robert C. Brewster*

Full article and list of author affiliations: https://doi.org/10.1126/science.adv2064

INTRODUCTION: Transcription factor (TF) function is important for the proper regulation of gene expression, and individual TFs can have very different effects on gene expression depending on the identity of the promoter that they regulate. This highlights the context-dependent nature of their regulatory roles. Traditionally, TFs have been classified as "activators" or "repressors" on the basis of their net effect on expression. However, this simplistic classification fails to explain why and how TFs can have distinct functions at different promoters and the contextual differences that influence TF function.

RATIONALE: Understanding how TF function is related to promoter identity is crucial for elucidating the mechanisms of gene regulation and enhancing our ability to predict TF function in different biological contexts. To interpret how TFs regulate gene expression across different promoters, we use a simplified thermodynamic model that predicts two possible, distinct relationships between TF function and the constitutive strength of promoters: Fold change increases or decreases with increasing promoter strength, depending on whether the TF has negative (destabilizing) or positive (stabilizing) interactions with RNA polymerase (RNAP), respectively. To reveal the relationship between TF function and promoter strength, we measured regulation by a single TF, with a regulatory context that was otherwise held constant, on promoters whose strength was altered systematically by both genetic and physiological perturbations.

RESULTS: For every TF tested, we find the same basic relationship between fold change and constitutive expression level. Each TF, both activators and repressors, exerts a lower fold change on stronger promoters. We find that the scaling between fold change and constitutive promoter strength obeys a precise inverse scaling relationship, as predicted by theory for TFs with stabilizing interactions. The precise scaling has a distinct implication: Promoters that differ in basal activity by orders of magnitude will have the same regulated level for a given TF, dictated by details such as TF identity and binding location. As such, TFs are predicted to have an innate property that buffers physiological or genetic perturbations to the promoter to maintain a steady level of regulated expression. We demonstrate this buffering across all TFs studied.

CONCLUSION: Among a diverse set of TFs, we see a universal relationship between fold change enacted by the TF and constitutive strength of the regulated promoter. This relationship is a useful fail-safe where a TF can adjust gene expression to buffer against perturbations and maintain homeostasis. □

*Corresponding author. Email: robert.brewster@umassmed.edu Cite this article as V. Parisutham *et al.*, *Science* **389**, eadv2064 (2025). DOI: 10.1126/science.adv2064

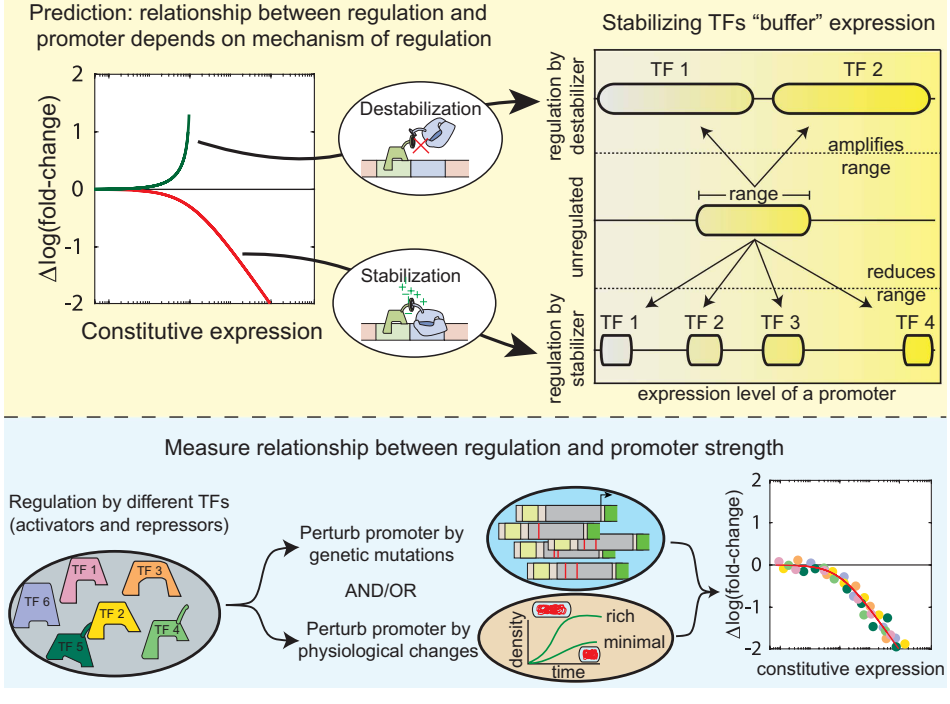

Mechanism of TF regulation. (Top) A general thermodynamic model predicts the relationship between fold change and the constitutive strength of the promoter regulated by a TF. The theory predicts two possible behaviors based on whether the TF has stabilizing (attractive or cooperative) or destabilizing (antagonistic or hindering) interactions with RNAP. TFs with destabilizing interactions are predicted to amplify the range of expression of a library of promoters, whereas TFs with stabilizing interactions would reduce that range. (Bottom) Experimental measurements of several TFs (both activators and repressors) on mutated libraries of promoters—in different media and with varying concentrations of polymerase—give a single relationship precisely aligned with that expected from TFs with stabilizing interactions.

MOLECULAR BIOLOGY

E. coli transcription factors regulate promoter activity by a universal, homeostatic mechanism

Vinuselvi Parisutham[1], Sunil Guharajan[2,3], Melina Lian[4], Md Zulfikar Ali[5], Hannah Rogers[1], Shannon Joyce[1], Mariana Noto Guillen[1], Robert C. Brewster[1]*

Transcription factors (TFs) may activate or repress gene expression through an interplay of different mechanisms, including RNA polymerase (RNAP) recruitment, exclusion, and initiation. However, depending on the regulated promoter identity, TF function can vary, and the principles underlying this context dependence remain unclear. We demonstrate an inverse scaling relationship between the promoter's basal activity and its regulation by a given TF. Specifically, activation is weaker and repression is stronger on stronger promoters. This scaling applies to both activators and repressors, which suggests a common underlying mechanism where TFs regulate expression by stabilizing RNAP binding at the promoter. The consequence of this relationship is that TFs buffer expression by affecting constant regulated expression levels across promoters of different basal activity, ensuring homeostatic control despite genetic or environmental changes.

Transcription factors (TFs) are crucial determinants of gene regulation, functioning through a myriad of regulatory mechanisms to ensure precise control of cellular processes. TFs bind to specific DNA sequences, often located near the genes that they regulate, and either promote or inhibit transcription. The regulatory mechanisms used by TFs are diverse and complex, and regulation may alter the rate of one or more steps in the multistep process between RNA polymerase (RNAP) binding and promoter clearance (*1*–*4*). The complexity of predicting the regulatory function of a specific TF in various genetic and physiological contexts arises from the propensity of TFs to regulate multiple steps of the transcription process combined with the intricate interplay of the number and types of TFs, their binding strengths, binding site locations, and promoter strength (*5*–*8*). In particular, TFs are usually classified on the basis of their net regulatory function (activation or repression) rather than their mechanisms of regulation. Because of this classification scheme, it may seem surprising that the same TF can have both activating and repressing interactions with different promoters, even in similar contexts. Examples of such interactions have been observed in both prokaryotic (*9*–*11*) and eukaryotic systems (*12*).

In this work, we measured the relationship between TFs and promoters in a controlled way in *Escherichia coli*. We systematically altered constitutive expression levels driven by a promoter through several methods, including altering the basal promoter sequence and perturbing physiological conditions, such as growth media or polymerase availability. Each perturbation altered the constitutive expression rate of the promoter while holding other TF-related features (such as TF identity, binding site position, and sequence) constant, thereby allowing us to confidently measure the relationship between TF function and promoter identity.

[1]Department of Systems Biology, UMass Chan Medical School, Worcester, MA, USA. [2]Division of Gastroenterology and Nutrition, Boston Children's Hospital, Boston, MA, USA. [3]Division of Pediatrics, Harvard Medical School, Boston, MA, USA. [4]Department of Chemistry, University of Southern California, Los Angeles, CA, USA. [5]Department of Geology, Physics and Environmental Science, University of Southern Indiana, Evansville, IN, USA. ***Corresponding author. Email: robert.brewster@umassmed.edu**

General gene regulation model to interpret TF-promoter relationship

To interpret the relationship between regulation and promoter strength, we use a simple thermodynamic model of gene regulation that we and others have proposed previously (*13*–*18*). In this model, regulation by a single TF is represented as activity on two steps of the transcription process (Fig. 1A). The first regulatory mechanism affects RNAP recruitment and stability at the promoter and is parameterized by β (a positive, real number); $\beta > 1$ corresponds to TFs with positive stabilizing or recruiting interactions with polymerase, and $\beta < 1$ corresponds to negative interactions with polymerase through effects such as steric hindrance. The second mechanism alters transcription initiation and promoter clearance and is parameterized by α (also a positive, real number). $\alpha > 1$ indicates TFs that increase the rate of transcription initiation, whereas $\alpha < 1$ indicates inhibition or slowing of this process. Thus, a value of α or β greater than 1 indicates up-regulation of a specific transcriptional step, whereas a value less than 1 indicates down-regulation. Historically, in vitro approaches studying TF function have attempted to determine which steps of the transcription process are regulated by a TF. A common model for proximally binding repressors is steric hindrance, where TF binding occludes RNAP binding to the promoter ($\beta < 1$ in our model). Various in vitro studies have identified steric hindrance as a mechanism of action for common repressors (*19*, *20*), including LacI (*21*, *22*). By contrast, activation is often attributed to positive recruiting interactions ($\beta > 1$ in our model) between specific TF domains and RNAP subunits (type I and II activation) (*23*).

We make no assumption a priori about which step or steps a TF will regulate; instead, the general model introduced in this work allows interpretation of TF function in vivo through the two mechanisms described above: stabilization or destabilization and acceleration or deceleration (*12*, *14*, *16*, *24*). The full, general thermodynamic model is derived in the supplementary text, section "Derivation of the general thermodynamic model" (fig. S1). However, the model can be simplified by considering saturating TF concentrations, so that TF-unbound states in the regulated condition can be ignored. The thermodynamic model makes a simple prediction for both the constitutive expression levels (C) and regulated expression levels (R) (Fig. 1B). The relationship between the fold change in gene expression at a saturating TF concentration (FC) and the constitutive expression level (C) is shown in Fig. 1C.

The qualitative nature of the relationship between FC and C is determined by whether the TF is stabilizing ($\beta > 1$) or destabilizing ($\beta < 1$). If a TF is stabilizing (TF-RNAP interactions are favorable, $\beta > 1$), it enacts lower fold change on stronger promoters (Fig. 1D). That is, repressors repress more (Fig. 1D, red line), and activators activate less on strong promoters (Fig. 1D, black line) compared with weaker ones. The opposite relationship is predicted if the interactions are destabilizing (TF-RNAP interactions are unfavorable, $\beta < 1$; Fig. 1E). A consequence of our model, which considers two mechanisms of regulation, is that a destabilizing TF can still activate and a stabilizing TF can repress, depending on the TF's role in the other step of transcription. Furthermore, the role (activation or repression) can be contingent on the strength of the promoter (see green line in Fig. 1, D and E).

Some conserved properties of these fold change curves can be seen by rescaling how we plot the theory. First, we normalize the fold change, FC, by the fold change in the weak promoter limit, $\mathrm{FC}(C \to 0) = \alpha\beta$. Figure 2A shows the relationship between this normalized fold change metric and constitutive expression C: As constitutive promoter activity increases, stabilizers reduce fold change whereas destabilizers increase it. Second, Fig. 2B shows that if we also rescale the constitutive promoter activity C to $|\beta - 1|C / C_{\max}$, all data are expected to collapse to one of two possible behaviors differentiated entirely by the nature of the TF's interactions with RNAP—i.e., whether the TF is a stabilizer or destabilizer. Within this figure, we define three regimes: weak regulation, strong destabilization, and strong stabilization. For weak regulation,

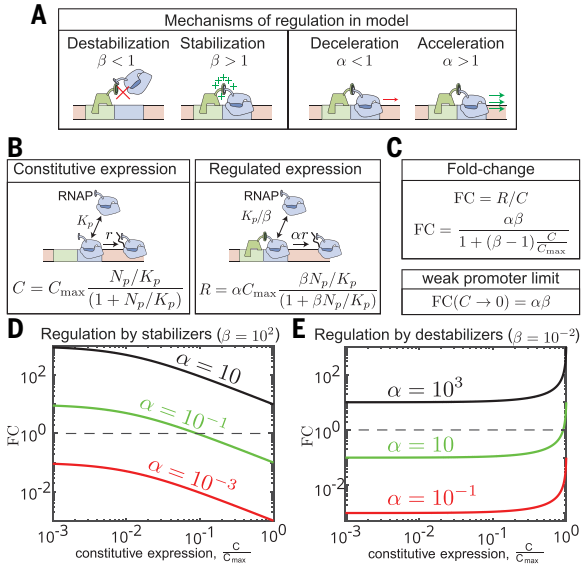

Fig. 1. Modeling promoter dependence of TF function. (**A**) A general thermodynamic model of TF function considers two distinct mechanisms: stabilization or destabilization and acceleration or deceleration. (**B**) Predicted expression from two conditions: constitutive (no TFs) and regulated (saturating TFs). (**C**) Fold change at saturating TF concentration (FC) from this model predicts a dependence on the constitutive expression level (C) of the regulated promoter. (**D**) Predictions for FC versus C for stabilizing TFs ($\beta > 1$) for a range of α. In all cases, FC decreases with promoter strength. (**E**) Predictions for destabilizing TFs ($\beta < 1$) show the opposite trend for any value of α.

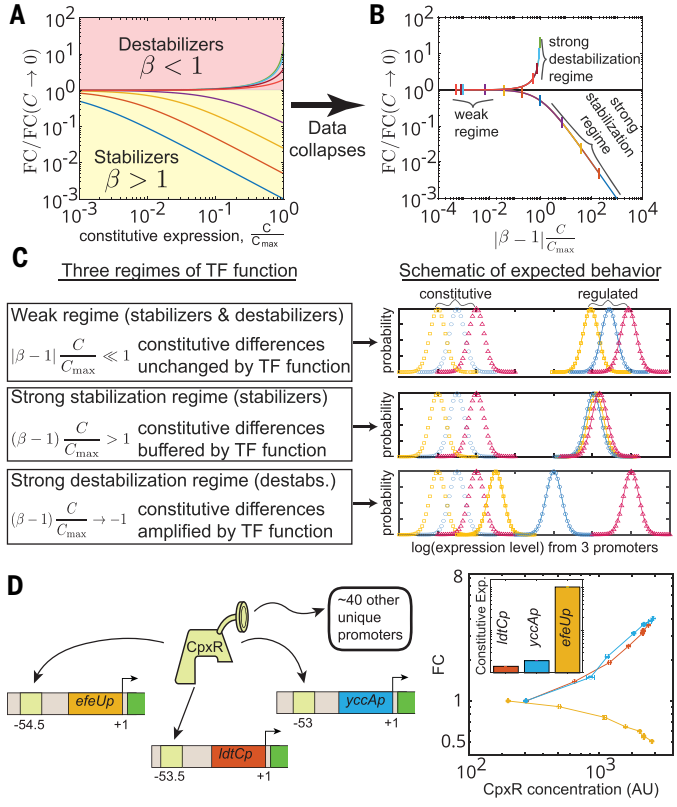

Fig. 2. Properties of the relationship between TF function and promoter strength. (**A**) Fold change, when normalized by the fold change of the weakest promoter $[FC/FC(C \to 0)]$, bifurcates into two behaviors based on the nature of TF-RNAP interactions ($\beta > 1$ or $\beta < 1$). (**B**) Renormalizing the constitutive promoter strength by $(\beta - 1)$ collapses all possible curves into only two distinct curves. These curves show different behaviors in three distinct regimes. (**C**) A schematic demonstrating the behavior of each regime in (B). The strong stabilization regime has a feature where differences in constitutive expression of the promoter are buffered by TF regulatory activity. (**D**) Example data for the TF CpxR on three natural promoters, regulated at similar relative binding positions on the promoter. The fold change is qualitatively different depending on which promoter is regulated by the TF. AU, arbitrary units.

where $|\beta - 1|C/C_{\max} \ll 1$, the fold change is insensitive to constitutive expression level of the promoter. Thus, any differences in constitutive expression level are expected to persist through to the regulated expression level and the fold change remains constant (Fig. 2C, top panel). The strong stabilization regime occurs when $(\beta - 1)C/C_{\max} > 1$ and is possible only for stabilizers ($\beta > 1$). This corresponds to a regime where fold change scales with the inverse of constitutive expression (C^{-1}). This produces a behavior, shown schematically in the middle panel of Fig. 2C, where stabilizing TFs elicit the same regulated level regardless of the constitutive expression of the promoter; if the constitutive expression doubles, the regulated level remains unchanged. Finally, for strongly destabilizing TFs $[(\beta - 1)C/C_{\max} \to -1]$, we expect TFs to drive divergent levels of regulated expression from promoters with relatively small differences in constitutive levels (Fig. 2C, bottom panel). This behavior is expected strictly for destabilizers. Although we have focused on saturating TF concentrations so far, even at subsaturating concentrations, we expect the same qualitative scaling behavior but with different scaling parameters that also depend on TF concentration and binding affinity (supplementary text, section "Data collapse for non-saturating TF concentration in the thermodynamic model," and fig. S2).

As an example of the complex dependence between TF regulatory function and promoter identity in endogenous promoters, consider the TF CpxR, which regulates more than 40 different promoters in *E. coli* (*25*). Figure 2D shows data for fold change as a function of CpxR concentration for three CpxR-regulated promoters (*ldtCp*, *yccAp*, and *efeUp*). These promoters have CpxR binding sites at approximately the same position relative to their transcription start site (TSS). However, two of these promoters are activated by CpxR (*ldtCp* and *yccAp*), whereas the other (*efeUp*) is repressed. Although some context-specific features [such as TSS, 5′ untranslated region (UTR), ribosomal binding site (RBS), etc.] differ between these three promoters, one notable difference is that each core promoter gives rise to substantially different constitutive (unregulated) expression levels. The inset in Fig. 2D shows the measured expression of each promoter in a CpxR knockout strain. CpxR activated the two weak promoters and repressed the stronger promoter, which had 100-fold higher constitutive expression. Previous studies have suggested that CpxR acts primarily through positive, stabilizing interactions with RNAP ($\beta > 1$) (*10*), which is qualitatively consistent with the trend seen in our data in Fig. 2D and with our prediction that a TF can switch from activating to repressing gene expression depending on core promoter strength. We do not require that the intrinsic function of the TF changes with promoter or is context specific; it is a basic expectation of our model. However, there are many uncontrolled aspects in the measurements in Fig. 2D. TF binds to slightly different positions on the promoter; the binding site sequences differ, and there may be differences in other regulatory factors involved at each endogenous promoter. Hence, we sought to measure the dependence of regulatory function on promoter strength in a system that controls these contextual confounds.

Measuring the relationship between TF function and promoter identity on a synthetic promoter library

We chose eight different TFs identified from a previous study (*16*) to examine the relationship between their regulatory effect and the

activity of the regulated promoter. These TFs were selected because of clear evidence of regulatory interactions on a synthetic promoter cassette that contained only a single binding site for the TF (*16*) (tables S1 and S2). An overview of the experimental method is outlined in Fig. 3A. To create a library of promoters with a spectrum of constitutive strengths, we mutated the −35 region of the promoter (153 possible combinations of single and double mutations; fig. S15) and randomly sampled 96 different clones. This library showed a range of constitutive expression levels varying from 100- to 1000-fold relative to the weakest promoter. We measured the expression of each promoter variant both in our library of inducible TF-mCherry strain (*24*) at maximum induction conditions (TF^{++}) and in a strain where the TF was deleted (TF^{-}). Ideally, TF^{++} conditions correspond to saturating TF levels, where further increase in TF concentration does not affect fold change. However, in some cases, regulation was at subsaturating TF levels (where the fold change had not plateaued) (fig. S4). In such cases, the scaling parameter depends on TF concentration and binding affinity. Nevertheless, this does not affect the overarching conclusions of our analysis (supplementary text, section "Data collapse for non-saturating TF concentration in the thermodynamic model"). It was also imperative to hold the TF concentration constant across all promoters. Unless otherwise stated, all TFs used in this study were fused with mCherry and expressed by an anhydrotetracycline (aTC)–inducible promoter. The mCherry tag did not perturb function (supplementary text, section "Influence of mCherry tag on TF function"). We then measured the fold change for each promoter and plotted it against the constitutive expression level of that promoter (Fig. 3B).

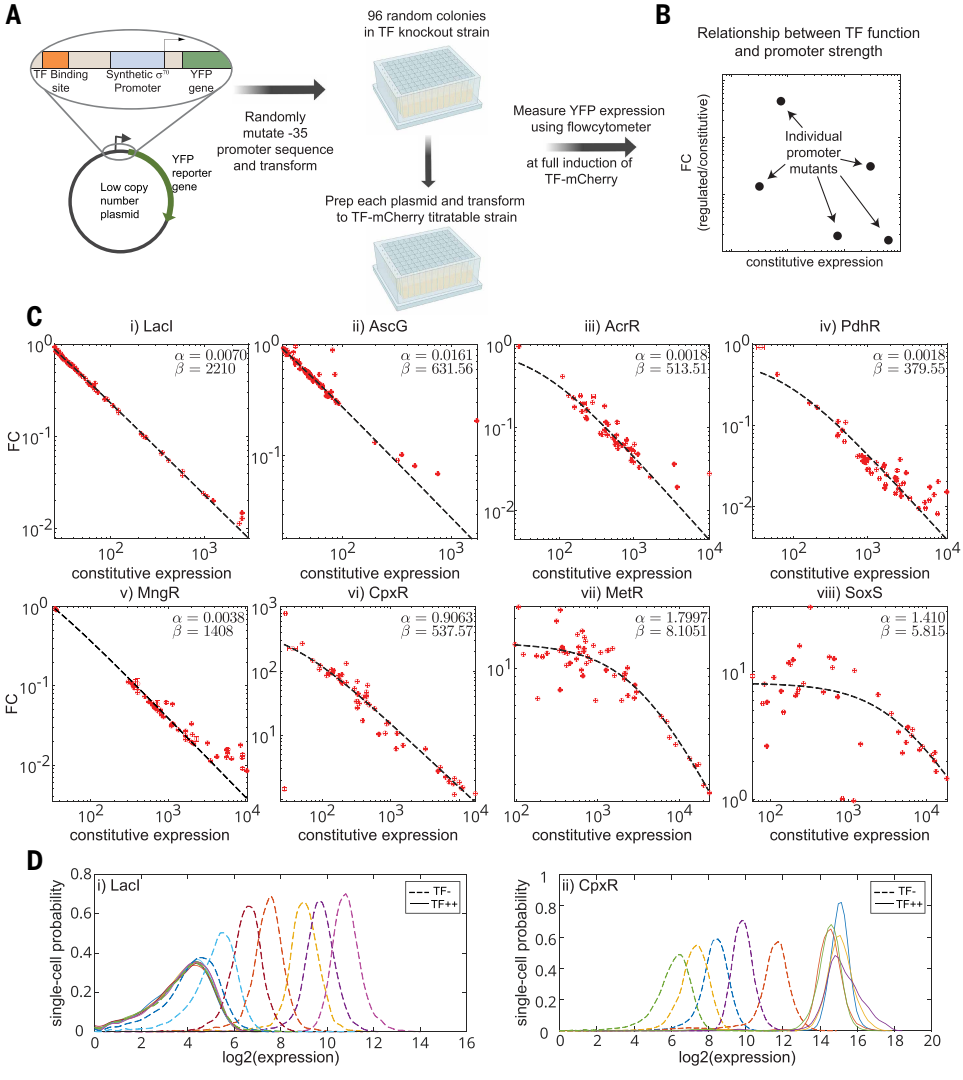

Fig. 3. Measuring the relationship between TF function and promoter activity for synthetic promoter variants. (**A**) Experimental approach to measure FC and *C* of random promoter variants. (**B**) Each data point in our plot represents the constitutive and regulated level of expression for one promoter variant. (**C**) For eight TFs measured here, the relationship between TF function and promoter strength conforms well to the predicted scaling of strong stabilizing interactions (black dashed lines). Subplots (i) to (iv) show TFs binding downstream of the promoter, and (v) to (viii) show TFs binding upstream of the promoter. Furthermore, panels (i) to (v) show TFs considered to be repressors and (vi) to (viii) show activators. (**D**) As expected from the theory for stabilizing TFs, the regulation by both CpxR and LacI causes a robust level of regulated expression from promoters with disparate constitutive levels of expression. Each color is a separate promoter variant for regulated (solid lines) and constitutive expression (dashed lines).

The data for the eight TFs are shown in Fig. 3C: five repressors (LacI, MngR, PdhR, AscG, and AcrR) and three activators (CpxR, MetR, and SoxS). The top row shows regulatory interactions for TFs with binding sites downstream of the promoter (centered between +11 to +16.5 from the TSS), and the bottom row features regulatory interactions from TFs with upstream binding site (centered between −52.5 to −64 from the TSS) (table S1). The dashed line in each plot shows a fit to the theory in Fig. 1C, with αβ and β as fit parameters. The maximum promoter activity, C_{max}, is set equal to the level of the promoter with the maximum expression in each dataset (range shown in fig. S6A). By setting C_{max} this way, we establish a lower bound on the maximum possible expression. Intuitively, if C_{max} increases, the value of β increases proportionally (fig. S6, B and C). Each of these eight TFs shows the predicted scaling relationship for stabilizing TFs, independent of function (activation or repression) or binding location on the promoter. However, for two activators, MetR and SoxS, the data for the weakest promoters fall into the regime where FC is constant with promoter strength, consistent with weaker stabilizing interactions, as indicated by lower β values from the fit.

A common model of repression assumes that regulation occurs solely through negative interactions with RNAP (steric hindrance) (*6*, *10*, *26*, *27*). In our general model, this corresponds to setting $\beta < 1$ and $\alpha = 1$. In this case, the model specifies that fold change at weak promoters equals β and fold change at strong promoters increases and eventually equals 1 for the strongest promoters. Our data show that neither of these predictions hold true. This contradicts the steric hindrance model, which fails to describe every repressive dataset in our study [Fig. 3C, panels (i) to (v)]. Furthermore, a purely decelerating mechanism ($\beta = 1$, $\alpha < 1$) also fails to explain our data, as we would expect a flat relationship between FC and *C*. In our model, to capture the observed inverse scaling of fold change with promoter strength, β

must be >1. Therefore, we conclude that there is a common positive interaction between TF binding and RNAP availability at the promoter in every regulatory interaction measured in this work. The net regulatory effect is determined by the magnitude of impact on the second step, transcription initiation (α in our model). This positive, stabilizing interaction may arise through direct interactions with RNAP; through indirect mechanisms, such as altering the DNA's local propensity to bind RNAP; or through transient rearrangements of TF binding state that are permissive to expression (*28*). In fig. S9, we summarize many previous studies on LacI function specifically and the implications of those results when interpreted through our model. The results from these studies are consistent with our findings. In the supplementary text, section "Data interpretation in the kinetic model framework for repressors" (figs. S7 and S8), we further discuss the implications of our results using a kinetic framework. In this framework, the limits of parameter regimes for stabilizing and destabilizing interactions depend on how promoter strength is altered—i.e., through changes in the RNAP on rate ($k_{p,\mathrm{on}}$) or off rate ($k_{p,\mathrm{off}}$) (*15*). Although the kinetic framework introduces greater complexity in interpretation, the central conclusion remains: $\beta > 1$ is essential to qualitatively account for our observations.

An important consequence of the stabilizing relationship seen for most TFs tested is that as constitutive expression levels change, the regulated levels remain constant for TFs with relatively high β values. This is demonstrated in Fig. 3D for two TFs, LacI and CpxR. We plot the single-cell distribution of constitutive (dashed lines) and regulated (solid lines) expression for several promoters (different colors in the plot) sampled from a 200-fold range of constitutive expression levels in the library. However, the corresponding measurements of the regulated expression levels (solid lines) varied by only roughly twofold. Thus, because of this inverse scaling relationship between TF function and promoter activity, the TF acts to buffer changes in expression from induced mutations in the promoter for both an activator and a repressor.

Measuring the relationship between TF regulation and promoter strength in different physiological conditions

The effect of physiological perturbations on constitutive expression has been studied using simple models that demonstrate the scaling between growth rate and constitutive expression (*29*, *30*). Despite the strong coupling between growth rates and transcription regulation, relatively little is known about how different TF functions are influenced by physiological perturbations (*30*). We measured the relationship between TF function and promoter strength by inducing changes to constitutive expression levels through physiological perturbation of growth rates using an array of carbon sources. We chose two TFs to examine: LacI and CpxR. We measured each promoter mutant library in six different minimal media conditions supplemented with a range of carbon sources that yielded doubling times between 55 (glucose) and 230 min (acetate). We anticipated that this would affect basal promoter activity by altering the concentration of crucial global regulators, including RNAP (*30*). One challenge from this approach is that the induced level of the TF of interest also changes with growth rate, possibly complicating a comparison of regulatory function across different media. Overall, TF concentrations were highest under slower growth conditions with pyruvate or acetate as the carbon source. Under saturating TF concentrations, where regulation becomes insensitive to changes in TF levels (as in the case of LacI; cyan data in fig. S4A), this change in concentration does not affect our findings. However, for TFs measured under subsaturating conditions (such as CpxR; brown data in fig. S4A), the TF concentration must be held constant across all media conditions (elaborated in supplementary text, section "Data collapse for non-saturating TF concentration in the thermodynamic model," and figs. S2 and S3). We used different inducer conditions to reach similar CpxR-mCherry signals across growth conditions for those experiments. We excluded the two slowest growth media (pyruvate and acetate), where the TF concentration was substantially higher than in other conditions, even after attempting to match TF levels. Including those data points (fig. S5B) shows the same scaling relationship but with a higher y intercept, as expected for increasing TF concentration in nonsaturating conditions.

Although changes in growth rate altered the fold change of the promoter library, the overall scaling relationship was preserved across the entire dataset for both TFs (Fig. 4A). The distribution of slopes from a straight-line fit of our theory for FC versus C for each promoter across different media for both CpxR and LacI is shown in Fig. 4B. Most promoters have a scaling relationship with a slope of −1 (see example in Fig. 4B, inset), consistent with what is expected from strong stabilization. This scaling relationship is observed both across individual promoters under varying growth rates and across the full promoter library within a single growth condition. This behavior remains consistent regardless of whether the perturbation is genetic or physiological and holds true for both activators and repressors. In Fig. 4C, we show the single-cell expression distribution for a single promoter across various growth rates. Although the constitutive expression level of the promoter depends strongly on growth rate, regulation is largely capable of buffering these changes where the stable level of expression is set by the identity of the TF regulating it; CpxR collapses the expression from the promoter into a higher expression state, whereas regulation by LacI also collapses the data but in a repressed state. Once again, by global perturbation to the constitutive expression through physiological changes, we find the same fundamental mechanisms of regulation that restore the regulated state expression level.

Promoter-TF relationship is predictive for regulation of alternative sigma factor promoters

We next developed a system to systematically perturb only the constitutive expression levels. The ideal way to do this would be to alter the availability of RNAP; however, limiting any core subunit of RNAP induces extreme physiological changes, which makes it difficult to isolate the effect on a specific gene of interest (*29*, *31*, *32*). Sigma factors are transiently associated subunits that confer promoter specificity to RNAP. *E. coli* encodes at least seven such variants, with σ^{70} being the primary sigma factor governing most genes. To circumvent the limitations of core RNAP perturbation, we designed a system to control the availability of an alternative sigma factor, σ^{28}, through expression from an inducible promoter—thereby allowing targeted and tunable control over constitutive promoter activity. Unlike σ^{70}, the σ^{28}-RNAP holoenzyme recognizes a limited set of promoters with a specific sequence. It regulates a subset of genes involved in flagellar synthesis (*33*–*37*), and the mechanisms of control (e.g., the anti-sigma factors, consensus promoter sequence, etc.) are well characterized (*38*, *39*). This system provides orthogonal control over both the physiological (through σ^{28}-RNAP concentration) and the genetic (through promoter sequence) components of the constitutive promoter activity.

We generated constructs with five different σ^{28} responsive promoters fused to yellow fluorescent protein (YFP). We induced expression using vanillic acid and additionally expanded the dynamic range of expression by performing these measurements in strains with and without anti-sigma factor *flgM*, which normally sequesters free σ^{28} and thereby reduces its availability for RNAP (*40*). The dashed lines in Fig. 4E, panel (i), show the range of constitutive expression for a single promoter at varying vanillic acid concentrations. The dashed lines in Fig. 4E, panel (ii), show the distribution of expression from each of the five promoters at an intermediate vanillic acid induction.

Regulatory measurements for the repressor LacI and the activator CpxR in the σ^{28}-inducible system are shown in Fig. 4D, panels (i) and (ii), respectively. Each promoter (represented by different colored points) was measured at eight different σ^{28} induction levels (with and without *flgM*). This setup allowed us to achieve constitutive expression levels spanning more than three orders of magnitude. Across this

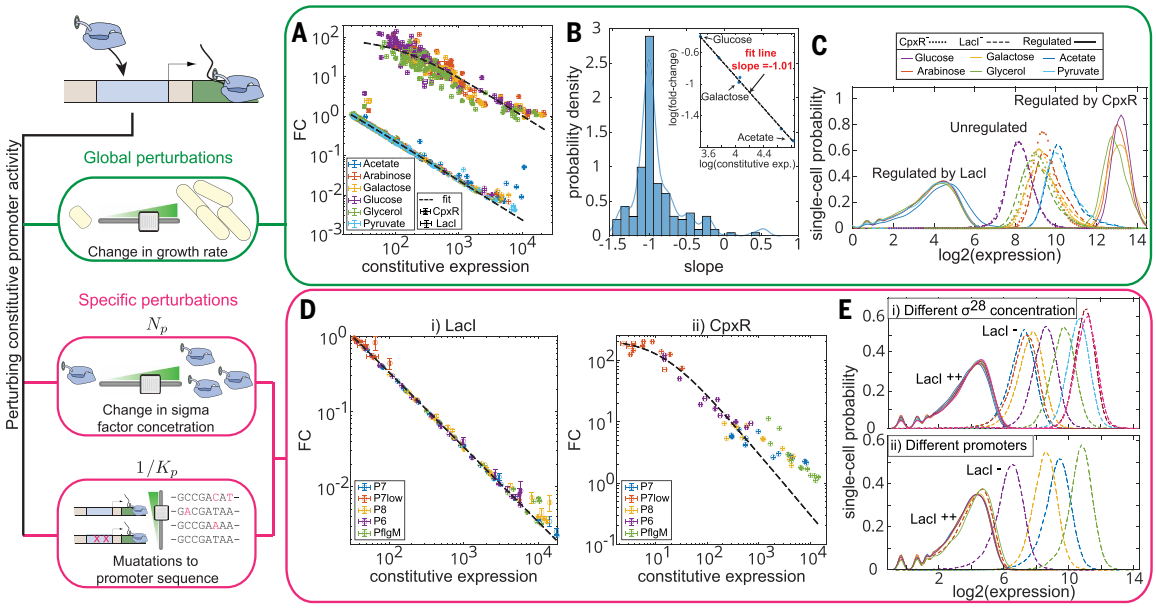

Fig. 4. Scaling of regulation is conserved across different methods of perturbations to constitutive expression. (**A**) Constitutive expression level altered through changes in the growth rate. The plot shows fold change against the constitutive level of expression for the promoter mutants regulated by LacI (circles) or CpxR (squares) when grown in media containing a variety of carbon sources (different colors). (**B**) Distribution of slope obtained from a linear fit of FC as a function of *C* for any single promoter in different media. Inset shows the straight-line fit to the data for one of the promoters grown in six different carbon sources. Most promoters show the expected relationship with slope −1. (**C**) Representative single-cell distribution of the fluorescence of unregulated (dotted lines) and regulated expression (dashed lines) across different growth media. Although this changes the constitutive expression levels of the promoter library, the regulated expression levels both for activation (CpxR) and repression (LacI) are relatively unchanged. (**D**) Perturbing constitutive expression through perturbation to RNAP concentration (through changes to σ^{28} concentration) or promoter sequence. Measurement of regulation by (i) LacI and (ii) CpxR for specific perturbations. Each color on the plot represents a different promoter, and each data point represents a fixed concentration of σ^{28}. (**E**) Single-cell distribution of regulated and constitutive expression for changing σ^{28} concentration [(i) different colors represent different vanillic acid concentration] or promoter strength [(ii) different colors represent separate promoters, as in (D) at 0.625 μM vanillic acid]. Perturbations in constitutive expression (dashed lines) produce relatively little change in the regulated expression level (solid lines).

range, fold change scaled consistently with a single set of α and β parameters for each TF, independent of whether expression was altered genetically or physiologically. Once again, we find that the data collapse when regulated by LacI for both physiological [Fig. 4E, panel (i)] and genetic perturbations [Fig. 4E, panel (ii)]. Different CpxR promoters do not align perfectly with theoretical predictions; however, within each promoter type, the inverse scaling relationship is preserved. This deviation may result from subsaturating levels of CpxR or limited σ^{28} availability.

Measuring the relationship between TF function and promoter identity in natural promoters

We observed a specific scaling relationship between TF function and constitutive promoter strength, which is pervasive in simple synthetic promoters designed to be regulated by a single TF. We extend this concept to determine whether this relationship holds true for naturally occurring promoters with complex regulatory architectures, such as DNA looping, multiple binding sites for the same TF, or interfering binding sites by other TFs. In Fig. 5A, we show measurements of several endogenous promoters regulated by the TF, SoxS (MarA and Rob, the other isoforms of SoxS are deleted from the strain to avoid any cross-talk): *poxBp* (yellow), *decRp* (blue), and *fldAp* (red) (*41*). These promoters were chosen because their endogenous binding sites are located at a similar position relative to the promoter (fig. S10A). We created 96 random mutants within each promoter using the same strategy as described above for the synthetic promoters. Unlike the synthetic promoters that have minimal differences between TFs, the natural promoters differ in every aspect, including the 5′UTR region, RBS, and TSS. These differences in translation efficiency and mRNA stability make it challenging to compare constitutive expression levels across different promoters. We measured the relative mRNA and protein expression levels for each of the three promoters and corrected the constitutive expression by normalizing to the ratio of mRNA to protein expression levels of each promoter (fig. S10B). This helped reduce nontranscriptional differences and enabled direct comparison of transcriptional activity. The effect of this multiplicative correction factor amounts to a horizontal translation of the data along the *x* axis and does not influence the scaling of any one dataset. The collection of promoter mutants showed regulation ranging from up to 70-fold activation down to threefold repression across the three promoters. Each promoter showed good agreement with the predicted scaling relationship of stabilizing interactions. The relationship is nearly universal across the three promoters over the entire range of fold change; however, fold change values for the *fldAp* promoter are systematically fourfold higher. This may result from slightly stronger regulatory interactions from SoxS at −61.5 compared with the other two positions (*16*) or from differences in SoxS binding site affinity across the three sites. Although measuring binding affinity is beyond the scope of this paper, we assessed the proximity of the annotated binding sites on *decRp*, *poxBp*, and *fldAp* to the SoxS consensus binding site using the TF PSSM browser in RegulonDB (*41*). This tool conducts a MEME analysis and generates *P* values for the annotated binding sequences. Lower *P* values indicate closer resemblance to the consensus sequence, and higher *P* values suggest similarity to a random sequence. We expect the SoxS binding sites of *decRp* and *poxBp* to be of similar strength (*P* values of 1.14×10^{-3} and 2.74×10^{-3}, respectively), whereas the site in *fldAp* is significantly closer to the consensus (*P* value of 1.76×10^{-4}) (*42*). Converting distance from consensus sequence to binding affinity

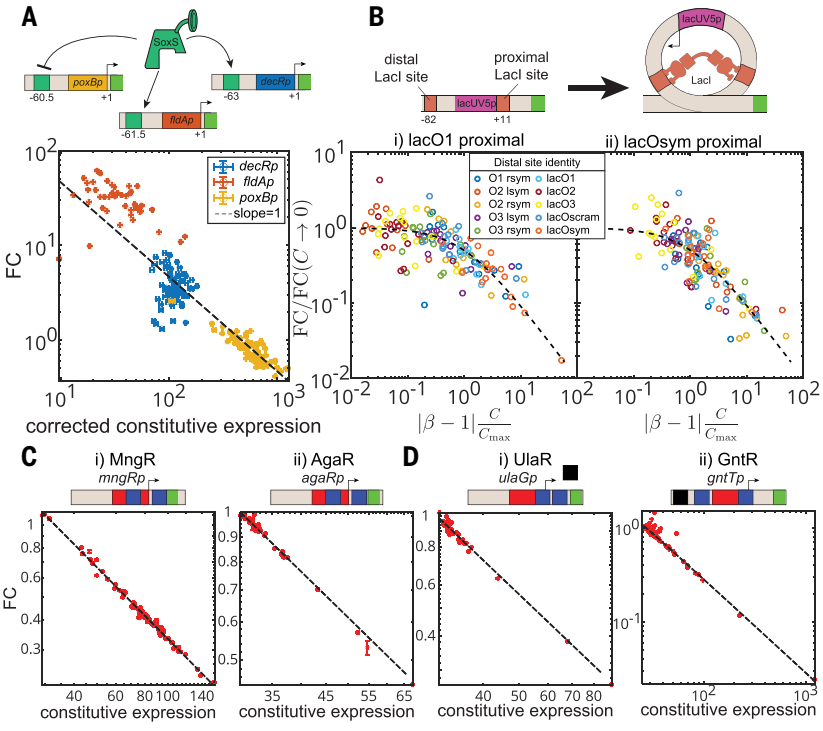

Fig. 5. Promoters with complex regulatory architecture show stabilizing relationship with mutant promoter library. (**A**) The top panel shows three native promoters of *E. coli* regulated by SoxS. The relative position of the binding site is shown as a complete green square with the center of the binding site marked underneath. The bottom panel shows the plot of fold change against the corrected constitutive expression level for the three native promoter mutant libraries. (**B**) The top panel shows a schematic representation of the DNA looping mediated regulation by LacI. The bottom panel shows the massively parallel reporter assay data from (*44*) plotted using uninduced or induced as a proxy for the fold change and induced expression as the constitutive expression. Data corresponding to the strong proximal binding sites [LacO1(i) and LacOsym (ii)] and all 10 different distal binding sites are plotted. (**C**) Measure of regulation for a promoter architecture with two binding sites for the TF of interest (dark blue squares) around the promoter (red square). (**D**) Measure of regulation for promoters with binding sites for other TFs (black squares) in addition to the binding site for the TF of interest.

is not straightforward, but this qualitatively supports the observed shift in *fldAp* data. Furthermore, we highlight that SoxS can switch roles from activation to repression simply by changing the strength of the core promoter. It is noteworthy that SoxS was previously thought to stabilize RNAP by acting as a co-sigma factor (*43*), which is consistent with our data. However, the ability to repress strong promoters implies that it must also repress transcription initiation or a downstream step.

Next, we explored a common natural regulatory architecture, DNA looping, where a TF binds to two sites on the promoter simultaneously to repress expression. Yu *et al.* (*44*) examined regulation by LacI using combinations of 10 different LacI binding sequences at both distal and proximal binding locations on a collection of promoters. In Fig. 5B, we show data with the two strongest sites (O1 and Osym) at the proximal position and any of the 10 sequences at the distal position. The spacing between these two LacI binding sites was designed to mimic the natural distance between O1 and O3 in the *lac* operon. Because the choice of the distal site influences the level of regulation and thus the model parameters, we fit each dataset to the theory and plotted all the data using the rescaled axes, as suggested in Fig. 1C. As shown, the data from every looping architecture collapse to a single curve and follow the expected scaling relationship for stabilizing interactions. This same relationship holds even for the weaker proximal sites, although regulation becomes very weak (fig. S11). Notably, one trend predicted by our theory and observed in the data is that stronger proximal sites shift the data toward the so-called strong stabilization regime, where fold change scales with the inverse of constitutive expression (fig. S11).

We further examined other TFs acting on endogenous promoters with more complex regulatory features where the mechanisms of regulation are unknown. Figure 5C shows two examples where regulation of the endogenous promoter occurs through two binding sites: (i) *mngRp* regulated by MngR and (ii) *agaRp* regulated by AgaR. Although these promoters are naturally wired for feedback, we deleted the endogenous TF genes, which allowed us to isolate the regulatory role under fixed, saturating TF concentrations. Figure 5D shows two additional natural promoters regulated by TFs that we have previously studied [UlaR and GntR (*16*)]. These promoters contain two binding sites for the controlled TF (UlaR or GntR) as well as additional TF binding sites; *ulaGp* includes an IHF binding site at an unknown location and *gntTp* features a CRP binding site. Again, in all cases, we find the same scaling relationship between fold change and constitutive promoter strength. Notably, these promoters, which are regulated by multiple TFs, show decreased response to promoter perturbations compared with synthetic promoters designed to be regulated by a single TF. This is in line with the idea that TFs can stabilize such genetic perturbations.

All data collapse to the same scaling law

To demonstrate the universal nature of this TF-promoter relationship in our measurements, we collapsed all the data from this study onto the same plot by rescaling the constitutive expression of each dataset by $(\beta-1)/C_{\max}$ and the fold change by $1/(\alpha\beta)$, akin to our theory plot in Fig. 2B (Fig. 6A). The data show a strong, universal collapse to the predictions of the stabilizing TF. We further added previously published datasets: from the activator AraC (*45*), from LacI looping (*44*), from the activator CRP (*46*), and from in vitro measurements of CarD from the bacterium *Mycobacterium tuberculosis* (*47*) (raw data are shown in figs. S11, S12, and S13). Across nearly six orders of magnitude in the fold change split between activation and repression (Fig. 6A, inset), the relationship between TF function and constitutive promoter strength collapses to a single functional form. This includes data from genetic perturbations, physiological perturbations, and in vitro measurements. In all cases, the data conform to a picture of TF regulatory function with a conserved regulatory mechanism.

This common relationship across all TFs studied in this work gives rise to a general buffering of regulated expression levels from promoters with varying activities. To visualize this buffering behavior across the diverse datasets in this study, we examined the magnitude of expression range in the promoter library (defined as the ratio of the highest expression level to the lowest expression level) for regulated and constitutive expressions (Fig. 6B). The minimum value of this range is 1, corresponding to identical expression across all promoters. Each data point represents one TF acting on a promoter library; blue points correspond to the entire library, and red points correspond to only those promoters in the strong stabilization regime $[(\beta-1)C/C_{\max}>1]$. The magnitude of buffering is demonstrated by a data point's perpendicular distance below the black dashed 1:1 line. In nearly all cases, regulation narrows the expression range of the full promoter library (blue points), and in all cases, it narrows the range for strong promoters (red points). The scale of buffering is typical on the order of 10- to 100-fold (between the red and green dashed lines). This behavior is most pronounced when considering only promoters in the strong

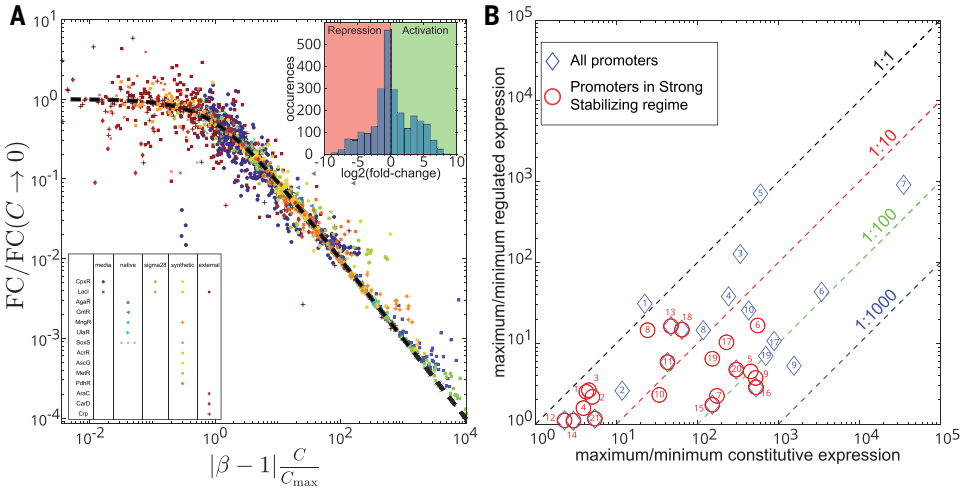

Fig. 6. Universal collapse for all regulation data. (**A**) All data from Figs. 3 to 5 are renormalized using the α and β obtained by fit to the theory in Fig. 1C. We also include data from previous studies (*44*, *45*, *47*), which we fit the same way. The black line represents the zero-parameter theory line, $f(x) = 1/(1+x)$. All data collapse to a single theory curve, suggesting a conserved universal mechanism of action between all measured regulations. The inset shows a histogram of FC values for all points included in the figure. (**B**) Scatter plot demonstrating the buffering of expression for each of our datasets. The dynamic range of expression in the library, defined as the ratio of expression level between the highest and lowest expression member of the library, for regulated expression against constitutive expression. Blue points represent the range across all promoters, and red points correspond to the range of promoters in the strong stabilizing regime $[(\beta-1)C/C_{max} > 1]$. Dashed lines indicate buffering levels: black, no buffering; red, 10-fold; green, 100-fold; blue, 1000-fold.

stabilization regime, where regulated expression rarely spans more than a 10-fold range. However, substantial buffering is also observed across the full promoter libraries. TF name, experimental condition, and a boxplot of promoter expression ranges for each dataset are shown in fig. S14 using the numerical labels from Fig. 6B.

Discussion

The relationship between TFs and the promoters that they regulate is an important determinant of gene expression levels. A given TF may regulate a battery of promoters with distinct features, and these promoters are regulated under various physiological conditions. Understanding the principles that govern how these features influence regulated gene expression is crucial for predicting how gene expression changes in response to mutation or environmental shifts and how these changes affect physiology. Using in vivo measurements in *E. coli* combined with a model of gene regulation, we discovered a universal principle that TFs function to stabilize RNAP at promoters and the fold change in expression enacted by strongly acting TF scales as the reciprocal of the constitutive activity of the promoter. This function applies to all TFs tested, both activators and repressors, acting on both synthetic and naturally occurring promoters. The relationship holds under perturbations to promoter strength through (i) random genetic mutations to the promoter, (ii) physiological changes to growth rate that affect transcriptional propensity, (iii) direct perturbation of RNAP availability, or (iv) any combination of these.

Every repressor measured in this study shows the same stabilizing relationship with promoter strength. This contrasts with the commonly accepted model of repressor action—steric occlusion that prevents RNAP from binding to the promoter in the presence of a repressor. This is sometimes called the competitive model of TF function. This idea has been supported by some in vitro studies, particularly for LacI (*21*, *48*). This model is intuitive because LacI binds very close to the *lac* promoter, with the 5′ end of the binding site at +1 on the promoter. However, conflicting in vitro studies have suggested that LacI regulates transcription initiation (*49*–*51*). Notably, Straney and Crothers found that LacI increased RNAP binding by more than 100-fold in their in vitro assays (*49*), although these contradictory results have sometimes been dismissed as artifacts of low ionic concentrations (*21*, *52*). Our in vivo findings support both conclusions by Straney and Crothers: (i) LacI negatively regulates transcription initiation and (ii) LacI positively affects RNAP stability at the promoter. In fact, we find this to be a general regulatory feature across all repressive TF-promoter interactions measured in our study. Our study does not find any evidence for regulation through steric occlusion, as inferred from our model. However, for some repressors, we observe slightly higher-than-expected fold changes at the strongest promoters. We suspect that this may relate to competitive rebinding of the promoter after DNA replication, a feature that would be most relevant for very strong promoters.

An important feature of stabilization interactions is that regulation is restorative by nature. Perturbations to the base level of gene expression, either through mutations to the promoter region or changes to the physiological state, which may up- or down-regulate global expression rates, are compensated when the TF-promoter interaction is stabilizing. By contrast, destabilizing TFs (which we do not find to be common) would exacerbate such perturbations. A speculative explanation for the prevalence of stabilizing interactions is that this robust relationship between TFs and promoters is evolutionarily favored; a TF that compensates for perturbations helps maintain stable expression levels and supports cellular homeostasis.

This observation of a conserved mode of regulation underscores the limitations of labeling TFs simply as activator or repressor and highlights the importance of understanding the mechanisms of regulation. If most TFs operate through stabilization, then many TFs (activators of weak promoters or repressors of strong promoters) may function as incoherent regulators (*10*, *12*, *14*–*16*, *53*), with their apparent role determined entirely by the basal strength of the promoters that they regulate.

Materials and methods

Bacterial strains

All strains used in this study are based on the collection of TF library strains described in Parisutham *et al.* (*24*), and synthetic reporters were from Guharajan *et al.* (*16*). Unless otherwise stated, all TFs used in this study were tagged with mCherry at the C terminus and controlled by adding anhydrous tetracycline (aTC). Reporters with native promoters were constructed by cloning the promoter sequence (starting from the TSS to include all the upstream regulatory regions of the promoter) upstream of the YFP reporter. For sigma factor titration, the regulator *vanR* and the promoter *vanCp* are polymerase chain reaction (PCR) amplified from the marionette strains (*54*) and combined by splice overlap extension PCR with a spectinomycin cassette and then inserted by lambda red recombinase into the native locus of *fliA* (the gene for σ^{28} sigma factor), replacing the native *fliAp* promoter with *vanCp*. The regulator *vanR*, was inserted bidirectionally to the *fliA* gene. The λ prophages carrying *Spec*^{R}*::vanCp::fliA* were transduced into the control and library strains of CpxR and LacI and selected for spectinomycin resistance. To introduce the anti-sigma factor knockout,

the λ prophage carrying the *flgM* knockout from the Keio collection was first transduced into the corresponding control strains, selected for kanamycin resistance, and then the kanamycin cassette was cured using the pCP20 plasmid. The λ prophages carrying the TF construct (library strain) and the *Spec*^{R}*::vanCp::fliA* constructs were then sequentially transduced into the control strains with the *flgM* knockout, through two tandem P1 transductions.

Creation of mutant library

Oligo pools homologous to the −35 region of the promoter were designed by replacing two of the wild-type sequences with random nucleotide "N" as depicted in fig. S15B. Fifteen oligos were designed for the −35 sequence, resulting in 154 possible combinations. For *DL5p*, the −35 region was selected from the literature (*16*). For native promoters, the −35 sequence was either based on the predictions in regulonDB (*41*) or the Salis promoter calculator (*55*). For synthetic *DL5p* constructs with the binding site located downstream of the promoter or for the native promoters, the reporter plasmids were PCR amplified with primers targeting regions immediately upstream and downstream of the −35 region. The single-stranded oligo pool with mutations was used as a bridge to complete the plasmid (fig. S15A). The PCR products were digested with DpnI, purified, assembled using NEB HiFi DNA assembly, and transformed into the corresponding control strains where the TF of interest was knocked out. For synthetic *DL5p* with binding sites located upstream, the forward primer carried mutations for the −35 region at the 5′ end, and the reverse primer was immediately upstream of the −35 region. The plasmid was blunt-end ligated using NEB's KDL reaction mix and transformed into the corresponding control. Ninety-six different clones per mutant library were sequenced to exclude misassembled constructs, and the remaining constructs were transformed into the corresponding library strain for further measurement.

Transformation to the library strains

Ninety-six independent colonies per mutant library were inoculated in 1 ml of LB media in deep-well plates and grown overnight. Cells were pelleted by centrifugation at 4000*g* for 30 min and suspended in P1, P2, and P3 buffers (Zymo) in a 1:1:2 ratio. Plates were centrifuged at 4000*g* for 30 min, and the supernatant is transferred carefully into three times the volume of absolute isopropanol to precipitate the plasmid. Plates were again centrifuged at 4°C for 1 hour at 1800*g*, isopropanol was decanted, and the plates were air-dried at room temperature for 3 to 4 hours. Fifty microliters of nuclease-free water was added to each well, and the plates were incubated at 42°C for 10 min to dissolve the plasmid. Plates were then incubated on ice with the chemically competent cells of the corresponding TF Library strains for 30 min, heat-shocked, and recovered in SOC for 1 hour. Plates were centrifuged again, and the pellet was resuspended in 30 μl of SOC and plated column-wise in LB-kanamycin plates using an eight-channel pipette. Plates were incubated overnight, and individual colonies are obtained.

Growth and fluorescence-activated cell sorting (FACS) measurement

Control and library strains of a given TF carrying promoter variants were grown overnight in 300 μl of LB with kanamycin and carbenicillin (chloramphenicol was also added for library strains). Cultures were diluted 1:5000 in 300 μl of M9 minimal media supplemented with glucose in 2-ml deep-well plates and grown at 37°C to an optical density (OD) of 0.2 to 0.5. The theoretical prediction in Fig. 1C is valid for saturated TF concentrations, effectively removing TF concentration as a variable. However, achieving true saturation may be challenging, particularly for weak binding sites. In this study, we approximate fully induced TF concentration (TF^{++}) as equivalent to saturated levels. This assumption does not substantially affect our conclusions, provided that TF concentration remains constant and relatively high. Except for SoxS, TFs were induced with 25 ng/ml aTC. SoxS was induced with 6 ng/ml aTC, as higher concentrations reduced cell growth. For MetR, comparisons were made between the uninduced library strain and 25 ng/ml aTC as the MetR knockout could not grow in M9 minimal media. For physiological perturbations, M9 minimal media was supplemented with different carbon sources (glycerol, galactose, L-arabinose, sodium pyruvate, or sodium acetate) to achieve different growth rates. Measurements for sigma factor variants were performed similarly to those for synthetic promoters, using M9 minimal media with glucose and 25 ng/ml aTC. Vanillic acid was serially twofold diluted, from 10 μM, to vary σ^{28} concentration. Strains were diluted 1:80 in M9 minimal media without a carbon or nitrogen source to arrest cells in a steady state and incubated on ice until measurement. Plates were measured for mCherry and YFP fluorescence using BD LSRFortessa with HTS (*X*–20–Model: 656385) and default high-throughput settings. mCherry was measured using a PE-CF594 laser at 600 V. For YFP, fluorescein isothiocyanate (FITC) voltage was optimized to distinguish autofluorescence from weak promoter signals (fig. S16, A and B). All YFP fluorescence was measured at 300 V of FITC. CST calibration was performed every day.

Data analysis and fitting to the model

Raw data were extracted from .fcs files using custom-built MATLAB code, and unsupervised gates were applied as described in (*27*). Mean and standard error were calculated for YFP fluorescence after subtracting autofluorescence. Samples with fewer than 5000 events were excluded (except for acetate, where the cutoff was 1000). Fold change was calculated as the mean ratio of fluorescence between library and control strains across two independent experiments. Data were then fit to the model with αβ and β as fit parameters and C_{max} set by the promoter mutant with the maximum fluorescence for a given TF. Cells with negative fluorescence were excluded only for visualization in single-cell fluorescence histograms.

Measuring translation differences for native promoters of SoxS

The highest constitutive mutant was selected from the promoter library for *decRp*, *fldAp*, and *poxBp*. The strains were grown as described above in multiple 300-μl wells, pooled at steady state (to a total of 1 ml), OD was quantified, and cell pellets were frozen overnight. Total RNA was isolated using the monarch RNA purification kit from NEB following the manufacturer's protocol. The resulting RNA was quantified using nanodrop and 2 ng/μl of total RNA was used in a single-step quantitative reverse transcription PCR (RT-qPCR) reaction with NEB's Luna RT-reagent. Separate reactions were set for the YFP and the kanamycin resistance gene. Both genes are expressed from the same reporter plasmid, and the kanamycin resistance gene serves as a housekeeping control for normalization. Reactions were performed with two biological and two technical replicates each. Standard curves for both kanamycin gene and YFP were prepared using the six dilutions of the plasmid. The concentration of YFP mRNA level was first normalized with the concentration of kanamycin mRNA and then by the total RNA yield per OD of the cell. This factor was then used to adjust all the constitutive expressions of the corresponding promoters.

REFERENCES AND NOTES

1. M. T. Record Jr., W. Reznikoff, M. Craig, K. McQuade, P. Schlax, in *Escherichia coli and Salmonella: Cellular and Molecular Biology*, F. C. Neidhardt, Ed. (ASM Press, 1996), pp. 792–821.
2. F. Zhang, J. M. Carothers, J. D. Keasling, Design of a dynamic sensor-regulator system for production of chemicals and fuels derived from fatty acids. *Nat. Biotechnol.* **30**, 354–359 (2012). doi: 10.1038/nbt.2149; pmid: 22446695
3. E. F. Ruff, M. T. Record Jr., I. Artsimovitch, Initial events in bacterial transcription initiation. *Biomolecules* **5**, 1035–1062 (2015). doi: 10.3390/biom5021035; pmid: 26023916
4. A. Barnard, A. Wolfe, S. Busby, Regulation at complex bacterial promoters: How bacteria use different promoter organizations to produce different regulatory outcomes. *Curr. Opin. Microbiol.* **7**, 102–108 (2004). doi: 10.1016/j.mib.2004.02.011; pmid: 15063844
5. J. Müller, S. Oehler, B. Müller-Hill, Repression of *lac* promoter as a function of distance, phase and quality of an auxiliary *lac* operator. *J. Mol. Biol.* **257**, 21–29 (1996). doi: 10.1006/jmbi.1996.0143; pmid: 8632456

6. H. G. Garcia, R. Phillips, Quantitative dissection of the simple repression input–output function. *Proc. Natl. Acad. Sci. U.S.A.* **108**, 12173–12178 (2011). doi: 10.1073/pnas.1015616108; pmid: 21730194
7. Y. Zhou, A. Kolb, S. J. Busby, Y. P. Wang, Spacing requirements for Class I transcription activation in bacteria are set by promoter elements. *Nucleic Acids Res.* **42**, 9209–9216 (2014). doi: 10.1093/nar/gku625; pmid: 25034698
8. J. Collado-Vides, B. Magasanik, J. D. Gralla, Control site location and transcriptional regulation in *Escherichia coli*. *Microbiol. Rev.* **55**, 371–394 (1991). doi: 10.1128/mr.55.3.371-394.1991; pmid: 1943993
9. D. Jensen, A. R. Manzano, J. Rammohan, C. L. Stallings, E. A. Galburt, CarD and RbpA modify the kinetics of initial transcription and slow promoter escape of the *Mycobacterium tuberculosis* RNA polymerase. *Nucleic Acids Res.* **47**, 6685–6698 (2019). doi: 10.1093/nar/gkz449; pmid: 31127308
10. S. Guharajan, S. Chhabra, V. Parisutham, R. C. Brewster, Quantifying the regulatory role of individual transcription factors in *Escherichia coli*. *Cell Rep.* **37**, 109952 (2021). doi: 10.1016/j.celrep.2021.109952; pmid: 34758318
11. E. A. Galburt, The calculation of transcript flux ratios reveals single regulatory mechanisms capable of activation and repression. *Proc. Natl. Acad. Sci. U.S.A.* **115**, E11604–E11613 (2018). doi: 10.1073/pnas.1809454115; pmid: 30463953
12. R. Martinez-Corral *et al.*, Emergence of activation or repression in transcriptional control under a fixed molecular context. bioRxiv 2024.05.29.596388 [Preprint] (2024). doi: 10.1101/2024.05.29.596388
13. H. G. Garcia *et al.*, Operator sequence alters gene expression independently of transcription factor occupancy in bacteria. *Cell Rep.* **2**, 150–161 (2012). doi: 10.1016/j.celrep.2012.06.004; pmid: 22840405
14. C. Scholes, A. H. DePace, Á. Sánchez, Combinatorial gene regulation through kinetic control of the transcription cycle. *Cell Syst.* **4**, 97–108.e9 (2017). doi: 10.1016/j.cels.2016.11.012; pmid: 28041762
15. M. Z. Ali, S. Guharajan, V. Parisutham, R. C. Brewster, Regulatory properties of transcription factors with diverse mechanistic function. *PLOS Comput. Biol.* **20**, e1012194 (2024). doi: 10.1371/journal.pcbi.1012194; pmid: 38857275
16. S. Guharajan, V. Parisutham, R. C. Brewster, A systematic survey of TF function in *E. coli* suggests RNAP stabilization is a prevalent strategy for both repressors and activators. *Nucleic Acids Res.* **53**, gkaf058 (2025). doi: 10.1093/nar/gkaf058; pmid: 39921566
17. L. Bintu *et al.*, Transcriptional regulation by the numbers: Models. *Curr. Opin. Genet. Dev.* **15**, 116–124 (2005). doi: 10.1016/j.gde.2005.02.007; pmid: 15797194
18. J. B. Kinney, A. Murugan, C. G. Callan Jr., E. C. Cox, Using deep sequencing to characterize the biophysical mechanism of a transcriptional regulatory sequence. *Proc. Natl. Acad. Sci. U.S.A.* **107**, 9158–9163 (2010). doi: 10.1073/pnas.1004290107; pmid: 20439748
19. E. Bertrand-Burggraf, S. Hurstel, M. Daune, M. Schnarr, Promoter properties and negative regulation of the *uvr*A gene by the LexA repressor and its amino-terminal DNA binding domain. *J. Mol. Biol.* **193**, 293–302 (1987). doi: 10.1016/0022-2836(87)90220-8; pmid: 3298658
20. F. Rojo, M. Salas, A DNA curvature can substitute phage phi 29 regulatory protein p4 when acting as a transcriptional repressor. *EMBO J.* **10**, 3429–3438 (1991). doi: 10.1002/j.1460-2075.1991.tb04907.x; pmid: 1655421
21. P. J. Schlax, M. W. Capp, M. T. Record Jr., Inhibition of transcription initiation by *lac* repressor. *J. Mol. Biol.* **245**, 331–350 (1995). doi: 10.1006/jmbi.1994.0028; pmid: 7837267
22. A. Sanchez, H. G. Garcia, D. Jones, R. Phillips, J. Kondev, Effect of promoter architecture on the cell-to-cell variability in gene expression. *PLOS Comput. Biol.* **7**, e1001100 (2011). doi: 10.1371/journal.pcbi.1001100; pmid: 21390269
23. G. Lloyd, P. Landini, S. Busby, Activation and repression of transcription initiation in bacteria. *Essays Biochem.* **37**, 17–31 (2001). doi: 10.1042/bse0370017; pmid: 11758454
24. V. Parisutham, S. Chhabra, M. Z. Ali, R. C. Brewster, Tunable transcription factor library for robust quantification of regulatory properties in *Escherichia coli*. *Mol. Syst. Biol.* **18**, e10843 (2022). doi: 10.15252/msb.202110843; pmid: 35694815
25. P. De Wulf, A. M. McGuire, X. Liu, E. C. Lin, Genome-wide profiling of promoter recognition by the two-component response regulator CpxR-P in *Escherichia coli*. *J. Biol. Chem.* **277**, 26652–26661 (2002). doi: 10.1074/jbc.M203487200; pmid: 11953442
26. R. C. Brewster *et al.*, The transcription factor titration effect dictates level of gene expression. *Cell* **156**, 1312–1323 (2014). doi: 10.1016/j.cell.2014.02.022; pmid: 24612990
27. M. Razo-Mejia *et al.*, Tuning transcriptional regulation through signaling: A predictive theory of allosteric induction. *Cell Syst.* **6**, 456–469.e10 (2018). doi: 10.1016/j.cels.2018.02.004; pmid: 29574055
28. E. Marklund *et al.*, Sequence specificity in DNA binding is mainly governed by association. *Science* **375**, 442–445 (2022). doi: 10.1126/science.abg7427; pmid: 35084952
29. S. Liang *et al.*, Activities of constitutive promoters in *Escherichia coli*. *J. Mol. Biol.* **292**, 19–37 (1999). doi: 10.1006/jmbi.1999.3056; pmid: 10493854
30. S. Klumpp, Z. Zhang, T. Hwa, Growth rate-dependent global effects on gene expression in bacteria. *Cell* **139**, 1366–1375 (2009). doi: 10.1016/j.cell.2009.12.001; pmid: 20064380
31. N. Shepherd, P. Dennis, H. Bremer, Cytoplasmic RNA Polymerase in *Escherichia coli*. *J. Bacteriol.* **183**, 2527–2534 (2001). doi: 10.1128/JB.183.8.2527-2534.2001; pmid: 11274112
32. S. Klumpp, T. Hwa, Stochasticity and traffic jams in the transcription of ribosomal RNA: Intriguing role of termination and antitermination. *Proc. Natl. Acad. Sci. U.S.A.* **105**, 18159–18164 (2008). doi: 10.1073/pnas.0806084105; pmid: 19017803
33. T. K. Kundu, S. Kusano, A. Ishihama, Promoter selectivity of *Escherichia coli* RNA polymerase sigmaF holoenzyme involved in transcription of flagellar and chemotaxis genes. *J. Bacteriol.* **179**, 4264–4269 (1997). doi: 10.1128/jb.179.13.4264-4269.1997; pmid: 9209042
34. B.-M. Koo, V. A. Rhodius, E. A. Campbell, C. A. Gross, Mutational analysis of *Escherichia coli* σ^{28} and its target promoters reveals recognition of a composite –10 region, comprised of an 'extended –10' motif and a core –10 element. *Mol. Microbiol.* **72**, 830–843 (2009). doi: 10.1111/j.1365-2958.2009.06691.x; pmid: 19400790
35. D. N. Arnosti, M. J. Chamberlin, Secondary sigma factor controls transcription of flagellar and chemotaxis genes in *Escherichia coli*. *Proc. Natl. Acad. Sci. U.S.A.* **86**, 830–834 (1989). doi: 10.1073/pnas.86.3.830; pmid: 2644646
36. R. M. Macnab, Genetics and biogenesis of bacterial flagella. *Annu. Rev. Genet.* **26**, 131–158 (1992). doi: 10.1146/annurev.ge.26.120192.001023; pmid: 1482109
37. X. Liu, P. Matsumura, Differential regulation of multiple overlapping promoters in flagellar class II operons in *Escherichia coli*. *Mol. Microbiol.* **21**, 613–620 (1996). doi: 10.1111/j.1365-2958.1996.tb02569.x; pmid: 8866483
38. O. A. Soutourina, P. N. Bertin, Regulation cascade of flagellar expression in Gram-negative bacteria. *FEMS Microbiol. Rev.* **27**, 505–523 (2003). doi: 10.1016/S0168-6445(03)00064-0; pmid: 14550943
39. C. Barembruch, R. Hengge, Cellular levels and activity of the flagellar sigma factor FliA of *Escherichia coli* are controlled by FlgM-modulated proteolysis. *Mol. Microbiol.* **65**, 76–89 (2007). doi: 10.1111/j.1365-2958.2007.05770.x; pmid: 17537210
40. L. G. Treviño-Quintanilla, J. A. Freyre-González, I. Martínez-Flores, Anti-Sigma Factors in *E. coli*: Common Regulatory Mechanisms Controlling Sigma Factors Availability. *Curr. Genomics* **14**, 378–387 (2013). doi: 10.2174/1389202911314060007; pmid: 24396271
41. H. Salgado *et al.*, RegulonDB v12.0: A comprehensive resource of transcriptional regulation in *E. coli* K-12. *Nucleic Acids Res.* **52**, D255–D264 (2024). doi: 10.1093/nar/gkad1072; pmid: 37971353
42. T. L. Bailey, C. Elkan, "Fitting a mixture model by expectation maximization to discover motifs in biopolymers," *Proceedings of the Second International Conference on Intelligent Systems for Molecular Biology* (AAAI Press, 1994), pp. 28–36.
43. I. M. Shah, R. E. Wolf Jr., Novel protein–protein interaction between *Escherichia coli* SoxS and the DNA binding determinant of the RNA polymerase α subunit: SoxS functions as a co-sigma factor and redeploys RNA polymerase from UP-element-containing promoters to SoxS-dependent promoters during oxidative stress. *J. Mol. Biol.* **343**, 513–532 (2004). doi: 10.1016/j.jmb.2004.08.057; pmid: 15465042
44. T. C. Yu *et al.*, Multiplexed characterization of rationally designed promoter architectures deconstructs combinatorial logic for IPTG-inducible systems. *Nat. Commun.* **12**, 325 (2021). doi: 10.1038/s41467-020-20094-3; pmid: 33436562
45. Y. Chen *et al.*, Tuning the dynamic range of bacterial promoters regulated by ligand-inducible transcription factors. *Nat. Commun.* **9**, 64 (2018). doi: 10.1038/s41467-017-02473-5; pmid: 29302024
46. T. L. Forcier *et al.*, Measuring cis-regulatory energetics in living cells using allelic manifolds. *eLife* **7**, e40618 (2018). doi: 10.7554/eLife.40618; pmid: 30570483
47. D. X. Zhu, C. L. Stallings, Transcription regulation by CarD in mycobacteria is guided by basal promoter kinetics. *J. Biol. Chem.* **299**, 104724 (2023). doi: 10.1016/j.jbc.2023.104724; pmid: 37075846
48. A. Sanchez, M. L. Osborne, L. J. Friedman, J. Kondev, J. Gelles, Mechanism of transcriptional repression at a bacterial promoter by analysis of single molecules. *EMBO J.* **30**, 3940–3946 (2011). doi: 10.1038/emboj.2011.273; pmid: 21829165
49. S. B. Straney, D. M. Crothers, Lac repressor is a transient gene-activating protein. *Cell* **51**, 699–707 (1987). doi: 10.1016/0092-8674(87)90093-6; pmid: 3315229
50. S. B. Straney, D. M. Crothers, Kinetics of the stages of transcription initiation at the *Escherichia coli lac* UV5 promoter. *Biochemistry* **26**, 5063–5070 (1987). doi: 10.1021/bi00390a027; pmid: 3311160
51. J. Lee, A. Goldfarb, *lac* repressor acts by modifying the initial transcribing complex so that it cannot leave the promoter. *Cell* **66**, 793–798 (1991). doi: 10.1016/0092-8674(91)90122-F; pmid: 1878972
52. F. Rojo, Repression of transcription initiation in bacteria. *J. Bacteriol.* **181**, 2987–2991 (1999). doi: 10.1128/JB.181.10.2987-2991.1999; pmid: 10321997
53. R. Martinez-Corral *et al.*, Transcriptional kinetic synergy: A complex landscape revealed by integrating modeling and synthetic biology. *Cell Syst.* **14**, 324–339.e7 (2023). doi: 10.1016/j.cels.2023.02.003; pmid: 37080164
54. A. J. Meyer, T. H. Segall-Shapiro, E. Glassey, J. Zhang, C. A. Voigt, *Escherichia coli* "Marionette" strains with 12 highly optimized small-molecule sensors. *Nat. Chem. Biol.* **15**, 196–204 (2019). doi: 10.1038/s41589-018-0168-3; pmid: 30478458
55. T. L. LaFleur, A. Hossain, H. M. Salis, Automated model-predictive design of synthetic promoters to control transcriptional profiles in bacteria. *Nat. Commun.* **13**, 5159 (2022). doi: 10.1038/s41467-022-32829-5; pmid: 36056029

ACKNOWLEDGMENTS

We thank M. Walhout, M. Razo-Mejia, and G. Chure as well as J. Dekker for helpful discussions. **Funding:** All authors were supported by the National Institute for General Medical Sciences (NIGMS) of the National Institutes of Health (NIH) under award no. R35GM128797. **Author contributions:** Conceptualization: V.P., S.G., M.Z.A., R.C.B.; Funding acquisition: R.C.B.; Investigation: V.P., M.L., H.R., S.J., M.N.G., R.C.B.; Methodology: V.P., M.L., H.R., S.J., M.N.G., R.C.B.; Project administration: V.P., R.C.B.; Supervision: M.Z.A., R.C.B.; Visualization: V.P., R.C.B.; Writing – original draft: V.P., R.C.B.; Writing – review & editing: V.P., R.C.B., S.G., M.Z.A., M.N.G. **Competing interests:** The authors declare no competing interests. **Data and materials availability:** All data are available in the main text or the supplementary materials.

SUPPLEMENTARY MATERIALS

science.org/doi/10.1126/science.adv2064
Supplementary Text; Figs. S1 to S18; Tables S1 and S2; References (*56*–*65*); MDAR Reproducibility Checklist; Data S1

Submitted 9 December 2024; accepted 13 June 2025

10.1126/science.adv2064